THE JOURNAL OF BIOLOGICAL CHEMISTRY
Vol. 277, No. 39, Issue of September 27, pp. 36449–36456, 2002

Printed in U.S.A.

The N-terminal Domains of Syntaxin 7 and vti1b Form Three-helix Bundles That Differ in Their Ability to Regulate SNARE Complex Assembly*[S]

Received for publication, May 6, 2002
Published, JBC Papers in Press, July 11, 2002, DOI 10.1074/jbc.M204369200

Wolfram Antonin, Irina Dulubova‡, Demet Araç‡, Stefan Pabst, Juliane Plitzner, Josep Rizo‡, and Reinhard Jahn§

From the Department of Neurobiology, Max-Planck Institute for Biophysical Chemistry, 37077 Göttingen, Germany and the ‡Departments of Biochemistry and Pharmacology, University of Texas, Southwestern Medical Center, Dallas, Texas 75390

The SNAREs syntaxin 7, syntaxin 8, vti1b, and endobrevin/VAMP8 function in the fusion of late endosomes. Although the core complex formed by these SNAREs is very similar to the neuronal SNARE complex, it differs from the neuronal complex in that three of the four SNAREs contain extended N-terminal regions of unknown structure and function. Here we show that the N-terminal regions of syntaxin 7, syntaxin 8, and vti1b contain well folded α-helical domains. Multidimensional NMR spectroscopy revealed that in syntaxin 7 and vti1b, the domains form three-helix bundles resembling those of syntaxin 1, Sso1p, and Vam3p. The three-helix bundle domain of vti1b is the first of its kind identified in a SNARE outside the syntaxin family. Only syntaxin 7 adopts a closed conformation, whereas in vti1b and syntaxin 8, the N-terminal domains do not interact with the adjacent SNARE motifs. Accordingly, the rate of SNARE complex assembly is retarded about 7-fold when syntaxin 7 contains its N-terminal domain, whereas the N-terminal domains of vti1b and syntaxin 8 have no influence on assembly kinetics. We conclude that three-helix bundles represent a common fold for SNARE N-terminal domains, not restricted to the syntaxin family. However, they differ in their ability to adopt closed conformations and thus to regulate the assembly of SNARE complexes.

SNARE[1] proteins play an essential role in all membrane fusion steps of the secretory and endocytic pathway (1, 2). They represent a superfamily of small membrane proteins that are distinguished by a conserved stretch of ~60 amino acids, referred to as the SNARE motif (3). Furthermore, most SNAREs possess a membrane anchor domain that is localized C-terminal of the SNARE motif. As monomers, SNARE motifs are unstructured (4, 5). When appropriate sets of SNARE motifs are mixed, they spontaneously assemble into tight bundles of α-helices, a reaction that is thought to tie membranes together and to initiate fusion. After fusion, SNARE complexes are disassembled by the chaperone-like ATPase *N*-ethylmaleimide-sensitive factor in conjunction with cofactors, thus reactivating the SNAREs for another round of membrane fusion (6).

Since assembly and disassembly of SNARE motifs is essential for fusion, major efforts have been made to understand these reactions in detail. From these studies, a few principles have emerged that appear to be valid for all SNAREs. First, SNARE complexes are represented by elongated four-helix bundles whose structure is remarkably conserved despite considerable sequence heterogeneity (7, 8). Each helix is contributed by a different SNARE motif, and each motif occupies a unique position in the four-helix bundle (9, 10). In the middle of the bundle is a highly conserved layer of four interacting polar side chains (three glutamines and one arginine), each contributed by one of the SNARE motifs. These observations led to their classification into Q- and R-SNAREs (7). Second, different SNAREs can be substituted for each other to a certain extent as long as they occupy equivalent positions (11–13). Third, assembly occurs spontaneously and is associated with the release of considerable amounts of energy (5, 14, 15). Indeed, liposome reconstitution experiments indicate that spontaneous assembly suffices to drive membrane fusion without the need for additional factors or for energy (16).

The finding that SNARE motifs are constitutively active raises the question of how they are regulated. Many SNAREs possess N-terminal extensions that represent independently folded domains. These domains have emerged as candidates for controlling the activity of the adjacent SNARE motifs. In the best studied examples, the neuronal syntaxin 1 and its yeast plasma membrane homologue Sso1p, the N-terminal domain consists of a three-helix bundle (17, 18) that interacts intramolecularly with the SNARE motif, resulting in an equilibrium between a "closed" and an "open" conformation (19–21). Since in the closed conformation the SNARE motif of syntaxin cannot bind to other SNAREs, the N-terminal domain can down-regulate the capability of syntaxin to form SNARE complexes. Indeed, removal of the N-terminal domain of Sso1p has been shown to accelerate SNARE complex assembly (22), and removal of this domain in syntaxin 1 accelerates SNARE-medi-

* This work was supported by Grant SFB 523 TP B6 from the Deutsche Forschungsgemeinschaft (to R. J.) and Grant NS37200 from the National Institutes of Health (to J. R.). The costs of publication of this article were defrayed in part by the payment of page charges. This article must therefore be hereby marked "*advertisement*" in accordance with 18 U.S.C. Section 1734 solely to indicate this fact.

[S] The on-line version of this article (available at http://www.jbc.org) contains a figure showing superimposed ^{1}H-^{15}N HSQC spectra of the full cytoplasmic region (*black contours*) and the isolated SNARE motif (*cyan contours*) of vti1b (*A*) and syntaxin 8 (*B*). The spectra of the full cytoplasmic regions were plotted at high contour levels to display only the sharpest cross-peaks, which correspond to the unstructured residues.

§ To whom correspondence should be addressed. E-mail: rjahn@gwdg.de.

[1] The abbreviations used are: SNARE, Q-SNARE, SNARE with glutamine in the 0 layer; R-SNARE, SNARE with arginine in the 0 layer; GST, glutathione *S*-transferase; TI-VAMP, toxin-insensitive vesicle-associated membrane protein; SM, Sec1/Munc18; Ni^{2+}-NTA, nickel-nitrilotriacetic acid; NOE, nuclear Overhauser effect; NOESY, NOE spectroscopy; HSQC, heteronuclear single quantum correlation; HNCACB, amide proton to nitrogen to α/β carbon correlation; CBCA(CO)NH, α/β proton to α/β carbon (via carbonyl carbon) to nitrogen to amide proton correlation.

ated liposome fusion (23). On the other hand, Munc18–1, a protein of the Sec1/Munc18 (SM) family, binds tightly to the closed conformation of syntaxin 1 and stabilizes it (19, 24). Thus, Munc-18–1 may serve as a negative regulator that prevents syntaxin from forming SNARE complexes, although undoubtedly it has an essential role in exocytosis (25). Hence, the N-terminal domains of SNAREs may serve as inhibitors of the adjacent SNARE motifs, operating by intramolecular interactions that sometimes may be controlled by other factors.

To what extent the properties summarized above are general or represent specializations of each SNARE is still under debate. First, the structures of the N-terminal domains are not conserved in all SNAREs. Vam3p and Sed5p, two additional yeast syntaxins, possess three-helix bundles in their N-terminal regions that are similar to those of syntaxin 1 and Sso1p (26, 27) However, the N terminus of Vam7p contains a Phox domain that appears to be unique for this SNARE and that is required for membrane attachment (28, 29). Also structurally different are the N-terminal domains of Sec22p (30) and Ykt6p (31). Both consist of a mixed α-helical/β-sheet profilin-like fold that, based on sequence alignments, may also be present in VAMP7 (also referred to as TI-VAMP). Second, it is unclear to which extent N-terminal domains interact with their respective SNARE motifs even if they have the same fold as syntaxin 1. In Sso1p, the domain binds to the SNARE motif even more tightly than in syntaxin 1 (22). In contrast, no such binding was observed in Vam3p (26). This difference may be explained by the fact that a surface groove that binds to the SNARE motif in Sso1p and syntaxin 1 is lacking in the Vam3p three-helix bundle. Of the N-terminal domains with different folds, that of Sec22b does not have an influence on the rate of SNARE assembly *in vitro* (30). In contrast, Ykt6p adopts a closed conformation that retards SNARE complex assembly (31). Third, the SM protein Sec1p does not bind to the closed conformation of Sso1p but rather to SNARE complexes containing Sso1p (32). In addition, the yeast syntaxins Sed5p and Ufe1p have recently been shown to bind to their corresponding SM protein, Sly1p, via a short peptide motif at the very N terminus of their sequence outside the three-helix bundle (27).

Previously, we have characterized a SNARE complex that mediates fusion of late endosomes (8, 9). Unlike the synaptic SNARE complex, in which only syntaxin 1 contains a large N-terminal region, three of the four SNAREs of the endosomal complex contain long N-terminal regions (syntaxin 7, vti1b, and syntaxin 8). In this study, we have determined whether these three SNAREs contain three-helix bundles in their N-terminal regions or include domains with different folds. Furthermore, we investigated whether the N-terminal domain of any of these SNAREs interacts with the SNARE motif and whether the presence of the N-terminal domain affects the rate of SNARE complex formation.

EXPERIMENTAL PROCEDURES

Material—2,2,2-trifluoroethanol was obtained from Merck. Expression constructs for the SNARE motifs of syntaxin 8 (residues 136–213), syntaxin 7 (residues 159–236), and vti1b (residues 130–206), as well as the cytoplasmic domain of syntaxin 7 (residues 1–236), were described before (9). Expression constructs for glutathione *S*-transferase (GST)-tagged endobrevin (residues 1–74) (11), vti1b (residues 1–207) (33), syntaxin 7 (residues 1–236), and syntaxin 8 (residues 1–213) (9) have been described previously.

Molecular Cloning—The cytosolic fragments of syntaxin 8 (residues 1–213), vti1b (residues 1–206), and endobrevin (residues 1–74), as well as N-terminal fragments of syntaxin 7 (residues 1–139), syntaxin 8 (residues 1–134), and vti1b (residues 1–124), were subcloned into the pET28a vector (Novagen, Madison, WI), which includes a thrombin cleavage site for the removal of the upstream His_6 tag. For the NMR studies of syntaxin 7, a cytosolic fragment (residues 2–235) or an N-terminal fragment (residues 2–131) were subcloned into the pGex-KT vector, which includes a thrombin cleavage site for the removal of the upstream GST tag. For PCR amplification, the following oligonucleotides were used: gagccacatatggccgcctccgcc and gccgctcgagttacttgttggttatcacttttc for vti1b (1–206), gaggcacatatggccccagacccc and ggaattctaggaagctgactttctgtcc for syntaxin 8 (1–213), gagccacatatggccgcctccgcc and ggcggcctcgagctattatcgattcaaatgctcgttc for the N-terminal domain of vti1b (1–124), gaggcacatatggccccagacccc and gcgcgcctcgagctattaccctagcctctggtctcc for the N-terminal domain of syntaxin 8 (1–134), ggcggcatatgtcttacactccggg and ggcggcctcgagctattactcttttgagctgtcttcag for N-terminal domain of syntaxin 7 (1–139), gaggcacatatggaggccagtgggag and cgaattctacttcacattcttccaccag for endobrevin (1–74), accggatcctacactccaggagttggtg and cagaattcttatctggatttgcgctgataat for syntaxin 7 (2–235), and accggatcctacactccaggagttggtg and ctgaattcaactgccagacactctgga for syntaxin 7 (2–131).

Purification of Recombinant Proteins and Cytoplasmic and Core Complexes—All recombinant proteins were expressed as His_6-tagged or GST-tagged fusion proteins. For NMR experiments, uniform ^{15}N or ^{13}C labeling was achieved by growing bacteria in minimal medium containing $^{15}NH_4Cl$ or [$^{13}C_6$]glucose as the sole nitrogen or carbon source, respectively. For all other experiments, standard bacteria media were used. Recombinant proteins were purified by Ni^{2+}-NTA agarose or GSH-Sepharose, respectively. Unless otherwise indicated, the tags of all His_6-tagged proteins were removed using thrombin. All proteins were further purified using Mono Q or Mono S columns on a fast protein liquid chromatography system (Amersham Biosciences). All proteins were 95% pure as judged by SDS-PAGE and Coomassie Blue staining. Assembly and purification of cytoplasmic and core complexes were done as described (9).

Binding Experiments—For the binding assays, purified recombinant proteins or preformed SNARE complexes (25 μM) were incubated for 10 h at 4 °C with His_6-tagged N-terminal domains of syntaxin 7, vti1b, and syntaxin 8 (5 μM) in 200 μl of incubation buffer (phosphate-buffered saline containing 20 mM imidazol and 1 mM phenylmethylsulfonyl fluoride). After incubation for 10 h at 4 °C, saturating amounts of Ni^{2+}-NTA-Agarose were added, and the samples were incubated for another 4 h at 4 °C. Protein in the unbound material was precipitated according to Wessel and Flügge (34). The beads were then washed eight times in incubation buffer except that the phenylmethylsulfonyl fluoride was omitted. Beads and 20% of the unbound material were analyzed by SDS-PAGE and Coomassie Blue staining.

Assembly Kinetics—To determine the influence of the N-terminal domains on the kinetics of complex assembly, the following samples were incubated: endobrevin (residues 1–74) and the three SNARE motifs of syntaxin 7 (residues 159–236), vti1b (residues 130–206), and syntaxin 8 (residues 136–213) (core complex); endobrevin (residues 1–74), the cytoplasmic domain of syntaxin 7 (residues 1–236) and the two SNARE motifs of vti1b (residues 130–206) and syntaxin 8 (residues 136–213) (sx7full complex); endobrevin (residues 1–74), vti1b (1–206), and the SNARE motifs of syntaxin 7 (residues 159–236) and syntaxin 8 (residues 136–213) (vti1bfull complex); endobrevin (residues 1–74), syntaxin 8 (1–213), and the SNARE motifs of syntaxin 7 (residues 159–236) and vti1b (residues 130–206)(sx8full complex); endobrevin (residues 1–74) and the three cytoplasmic regions of syntaxin 7 (residues 1–236), vti1b (residues 1–206), and syntaxin 8 (residues 1–213) (full complex). Each incubation was performed in 40 mM sodium phosphate/150 mM NaCl, 1 mM dithiothreitol at 5 °C with 20 μM of each component. At indicated time points, aliquots were taken, urea was added to a final concentration of 4 M, and the samples were analyzed by anion-exchanged chromatography using a Mono Q column on a SMART system (Amersham Biosciences). The amount of formed complexes at each time point was quantified as the integral under the peak corresponding to the complexes of the absorption profile at 280 nm. All measurements were performed in duplicates, and each peak integral was normalized to the average of the four peak integrals of the last two time points for each complex (150 and 300 h for core, vti1bfull, and sx8full complexes and 200 and 300 h for sx7full and full complexes).

NMR Spectroscopy—All NMR experiments were acquired at 25 °C on Varian INOVA500 or INOVA600 spectrometers. ^1H-^{15}N heteronuclear single quantum correlation (HSQC) spectra were acquired with samples containing 0.1–0.2 mM protein dissolved in the following buffers: 20 mM Tris-HCl, 150 mM NaCl, 1 mM EDTA, 1 mM dithiothreitol, 0.1 mM phenylmethylsulfonyl fluoride, pH 7.4, for syntaxin 7 and syntaxin 8 constructs and comparison of the N-terminal domain (residues 1–124) of vti1b and cytoplasmic domain (residues 1–206). The pH was decreased to 6.0 for comparison of the SNARE motif (residues 130–206) with the cytoplasmic region of vti1b. Backbone assignments for the syntaxin 7 N-terminal fragment (residues 2–131) and the vti1b N-

terminal fragment (residues 1–124) were obtained using ^{1}H-^{15}N three-dimensional NOESY-HSQC, HNCO, HNCACB, and CBCA(CO)NH experiments acquired on samples containing 0.7 mM protein. The NOESY-HSQC spectra were also used to assign selected NOEs that verified the secondary structure of the fragments.

Other Methods—Routinely, SDS-PAGE was carried out as described by Laemmli (35). Multiangle laser light scattering measurements were performed in 20 mM Tris-HCl, 150 mM NaCl, 1 mM EDTA, 1 mM dithiothreitol, pH 7.4, as described (11). Far UV CD spectra were recorded by averaging over 20 scans using steps of 0.2 nm with a scan rate of 50 nm/min on a JASCO model J-715U equipped with a Peltier element. Measurements were performed in Hellma quartz cuvettes with path lengths of 0.1 cm. All CD spectra were recorded after reaching equilibrium following an overnight incubation at 4 °C in 40 mM sodium phosphate, 150 mM NaCl, 1 mM dithiothreitol, pH 7.4. To evaluate changes of the CD spectrum attributable to domain interactions, the spectra were compared with the theoretically noninteracting sum of the individual spectra using the equation $[\Theta]_{sum} = \Sigma_i c_i n_i [\Theta]_i / \Sigma i\, c_i n_i$, where the c_i values are the respective concentrations of the proteins, the n_i values are the respective numbers of amino acid residues, and the $[\Theta]_i$ values are the mean residue ellipticities of the individual proteins. For thermal melts, the ellipticity at 222 nm was measured between 10 and 100 °C with a temperature increment of 25 °C/h. Percentage of α-helical content was calculated according to Chen *et al.* (36).

RESULTS

Circular Dichroism Reveals the Presence of Helical Domains in Syntaxin 7, Syntaxin 8, and vti1b—The endosomal SNARE complex investigated here contains the three Q-SNAREs syntaxin 7, syntaxin 8, vti1b, and the R-SNARE endobrevin/VAMP-8. We have shown previously that the four SNARE motifs form a SNARE complex with remarkable similarities to the neuronal SNARE complex (8, 9) with endobrevin corresponding to synaptobrevin 2, syntaxin 7 corresponding to syntaxin 1, and vti1b and syntaxin 8 corresponding to the N- and C-terminal SNARE motifs of SNAP-25, respectively. Furthermore, syntaxin 7, syntaxin 8, and vti1b contain N-terminal extensions that are not homologous to each other or to other SNAREs. These N-terminal extensions are resistant to limited proteolysis and thus are likely to represent independently folded domains (9).

For initial characterization, the bacterially expressed N-terminal domains of syntaxin 7 (residues 1–139), syntaxin 8 (residues 1–134), and vti1b (residues 1–124) were purified to homogeneity and analyzed by CD spectroscopy. As exemplified by the spectrum of the N-terminal domain of syntaxin 7 (Fig. 1*A*, Table I), all N-terminal domains showed a high α-helical content (around 60% for syntaxin 7, 71% for vti1b, and 77% for syntaxin 8). Addition of trifluoroethanol to a final concentration of 50% (v/v) did not increase the α-helical content. In contrast, trifluoroethanol induced α-helicity in the corresponding purified SNARE motifs (Fig. 1*A*, Table I), which are known to be unstructured as monomers (9). Thermal denaturation experiments with the N-terminal domains revealed steep unfolding transitions, supporting the conclusion that these fragments indeed represent independently folded and single domains (Fig. 1*C*).

Next, we tested whether the purified recombinant proteins are monomeric in solution. Some SNARE proteins such as yeast Vti1p are known to oligomerize (37), which would interfere with CD spectroscopy. However, size exclusion chromatography in combination with multiangle laser light scattering revealed that the N-terminal domains as well as the cytoplasmic fragments of syntaxin 7, vti1b, and syntaxin 8 are monomeric and correspond well to the calculated masses (Table II).

To examine whether the free N-terminal domains interact with their corresponding SNARE motifs, we recorded CD spectra of equimolar mixtures of the N-terminal domains and the SNARE motifs of syntaxin 7, vti1b, and syntaxin 8. In all cases, the α-helical contents equaled the sum of the individual domains (Table I). To confirm that the N-terminal regions do not interact with the free SNARE motifs or with the entire cytoplasmic region of the endosomal SNAREs, His_6-tagged versions of the N-terminal domains of syntaxin 7, vti1b, and syntaxin 8 were incubated with untagged and purified proteins corresponding to these regions followed by adsorption to Ni^{2+}-NTA agarose. No interaction of the N-terminal domains was observed with any of these recombinant proteins (Fig. 2 for syntaxin 7; data not shown for syntaxin 8 and vti1b). Similarly negative results were obtained when we tested for binding to preassembled endosomal SNARE complexes or to N-terminal domains of the partner SNAREs (Fig. 2 and data not shown). In addition, no binding of individual domains was detectable when the complete cytoplasmic domains of endobrevin, syn-

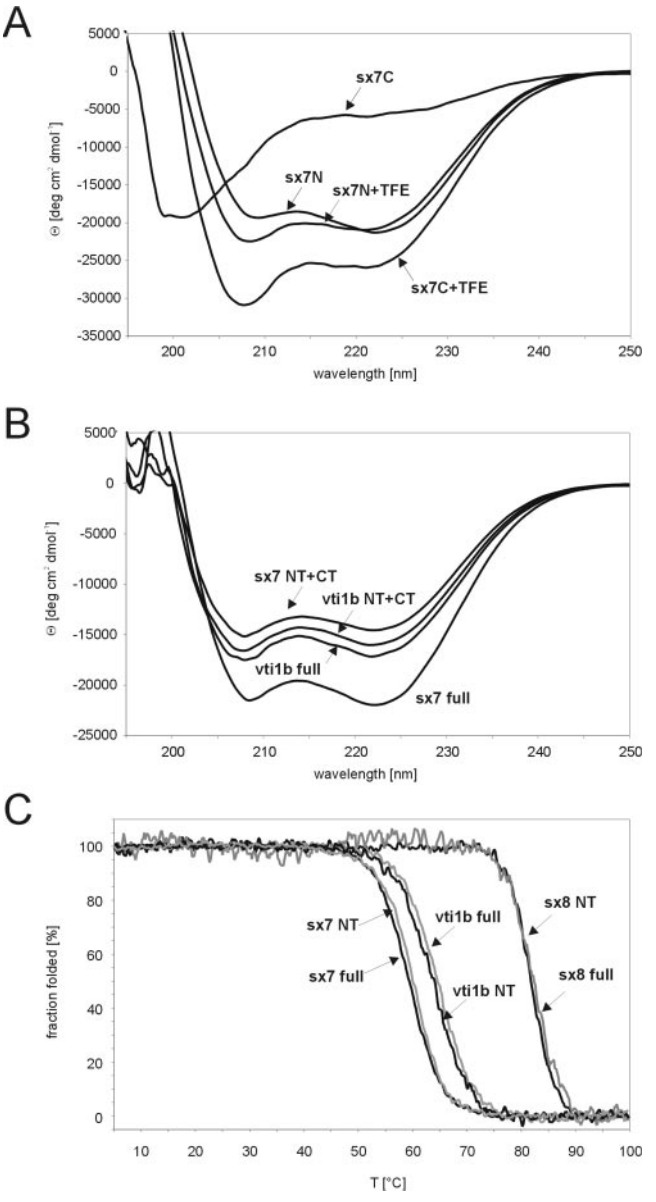

FIG. 1. **Structural characterization of individual domains in syntaxin 7, syntaxin 8 and vti1b and their interactions.** *A*, CD spectra of the N-terminal (*N*) and C-terminal (*C*) domains of syntaxin 7 in the presence and absence of 50% trifluoroethanol (*TFE*). *B*, CD spectra of the cytoplasmic regions of syntaxin 7 and vti1b and an equimolar mixture of the N-terminal and C-terminal domains (*NT*+*CT*) of syntaxin 7 and vti1b. *C*, thermal melting curves of the N-terminal domains (*gray*) and cytoplasmic domains (*black*) of syntaxin 7, vti1b, and syntaxin 8. Percentage of α-helical structure of the fragments as a function of temperature is shown. Change in the ellipticity at 222 nm was monitored, and the α-helical content was calculated.

TABLE I

α-helical content of fragments derived from endosomal SNAREs in the absence and presence of 50% trifluoroethanol

Cytoplasmic (eb, sx7 full, vti1b full, sx8 full), N-terminal (NT), C-terminal (CT), and equimolar mixtures of N-terminal and C-terminal (NT + CT) domains were analyzed by CD spectroscopy. α-helical content as well as the fraction of helix times the number of residues of the fragment (f^*n) are given. For the mixtures of N-terminal and C-terminal domains, the theoretically non-interacting values calculated from the observed spectra of the individual fragments are given in parentheses. TFE, trifluoroethanol.

	Θ_{222}	α-helical content	f^*n	Θ_{222}
		%		*50% TFE*
eb	−4,300	12.2	9.4	−26,600
sx7full	−22,000	61.1	146.1	−26,700
vti1bfull	−17,300	48.3	101.0	−26,300
sx8full	−17,000	47.5	102.6	−24,100
sx7 NT	−21,300	59.9	85.0	−20,800
vti1b NT	−25,200	70.9	90.1	−23,500
sx8 NT	−27,600	77.4	106.0	−25,400
sx7 CT	−6,000	17.1	14.0	−25,900
vti1b CT	−3,500	10.1	8.1	−25,700
sx8 CT	−5,500	15.5	12.7	−22,900
sx7 NT + CT	−14,700 (−15,700)	40.9 (44.2)	91.6 (99.0)	−24,400
vti1b NT + CT	−16,100 (−16,100)	44.8 (47.2)	93.2 (98.2)	−16,100
sx8 NT + CT	−18,800 (−19,300)	52.4 (54.2)	114.8 (118.8)	−25,000

TABLE II

Comparison of the molecular mass of the N-terminal domains and cytoplasmic fragments of endosomal SNAREs determined by multiangle laser light scattering and the theoretical weights of the fragments

Analyzed fragment	Theoretical mass	Measured mass
	kDa	*kDa*
sx7 NT[a]	15.8	13.8 ± 0.3
vti1b NT	14.2	13.3 ± 0.2
sx8 NT	15.7	11.6 ± 0.3
sx7 full	27.3	25.8 ± 0.3
vti1b full	25.8	25.4 ± 0.5
sx8 full	30.6	29.3 ± 0.4

[a] NT, N-terminal fragments.

taxin 7, vtib, and syntaxin 8 were used as a bait (data not shown).

The experiments described so far show that none of the N-terminal domains interact with the corresponding SNARE motifs or with any other constituent of the endosomal SNARE complex when binding is measured in solution between separately expressed domains. However, it cannot be ruled out that an intramolecular interaction may have been missed because the N-terminal domains and the adjacent SNARE motifs may bind in an intramolecular interaction that is too weak to be uncovered in such binding assays. Furthermore, in the closed conformation, the connecting region may contain secondary structural elements (*e.g.* α-helices such as in syntaxin and Sso1p (21, 24)) that are destroyed by the cleavage into two fragments.

As an initial test for such interactions within the full cytoplasmic regions of syntaxin 7, vti1b, and syntaxin 8, we compared the α-helical contents of the entire cytoplasmic portions with those of equimolar mixtures of the respective individual components, *i.e.* the SNARE motifs and the N-terminal domains. Although the helical contents of vti1b and syntaxin 8 resembled those of the corresponding mixtures (around 50%), the α-helical content of the cytoplasmic region of syntaxin 7 was higher than predicted from the sum of the individual values of the N-terminal domain and the SNARE motifs (60 *versus* 40%, Fig. 1*B*). Although the corresponding melting temperatures were identical (Fig. 1*C*), this difference suggests that the presence of the N-terminal domain induces structure in the SNARE motif of syntaxin 7.

NMR Analysis Shows That Syntaxin 7 and vti1b Contain Three-helix Bundle N-terminal Domains, but Only Syntaxin 7 Adopts a Closed Conformation—NMR spectroscopy showed that syntaxin 1 contains an autonomously folded three-helix

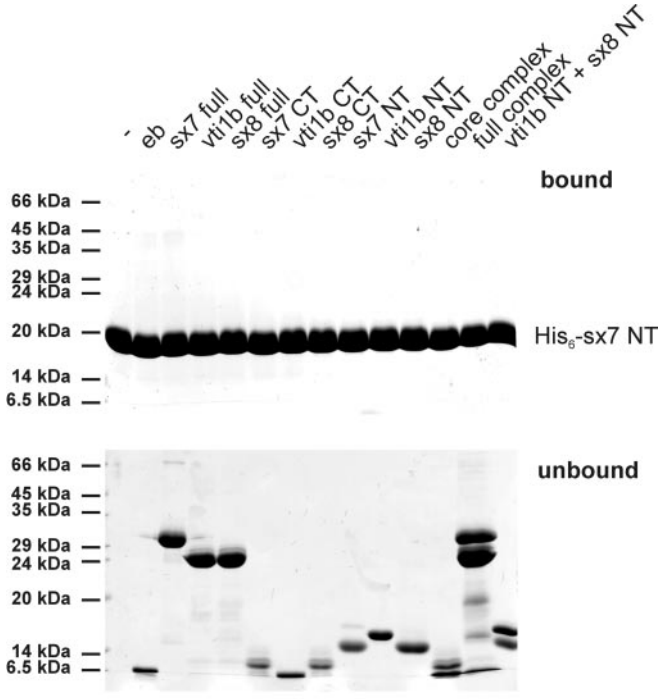

FIG. 2. **No Binding of endosomal SNAREs or domains within to the N-terminal domains.** His_6-tagged N-terminal domains of syntaxin 7 were incubated with the respective fragments. Bead bound material (*upper panel*, *bound*) and 20% of unbound material (*lower panel*, *unbound*) were analyzed by SDS-PAGE and stained with Coomassie Blue. *NT*, N-terminal; *CT*, C-terminal; *eb*, endobrevin.

N-terminal domain that folds back onto the SNARE motif to form a closed conformation (17, 19). Furthermore, the yeast vacuolar syntaxin Vam3p also contains a three-helix N-terminal domain but does not exhibit a closed conformation (26). Because of the limited sequence similarities between the N-terminal regions of syntaxins, it is difficult to predict with confidence whether syntaxin 7 contains a three-helix N-terminal domain. In addition, it is unclear whether the N-terminal domains of the SNAP-25 homologues vti1b and syntaxin 8 adopt a similar fold. To gain further insights into the structure of the N-terminal domains and their potential association with the SNARE motifs, we analyzed purified N-terminal domains of syntaxin 7, syntaxin 8, and vti1b, as well as their entire cytoplasmic regions, using NMR spectroscopy. In particular, we made extensive use of ^1H-^{15}N HSQC spectra. Such spectra

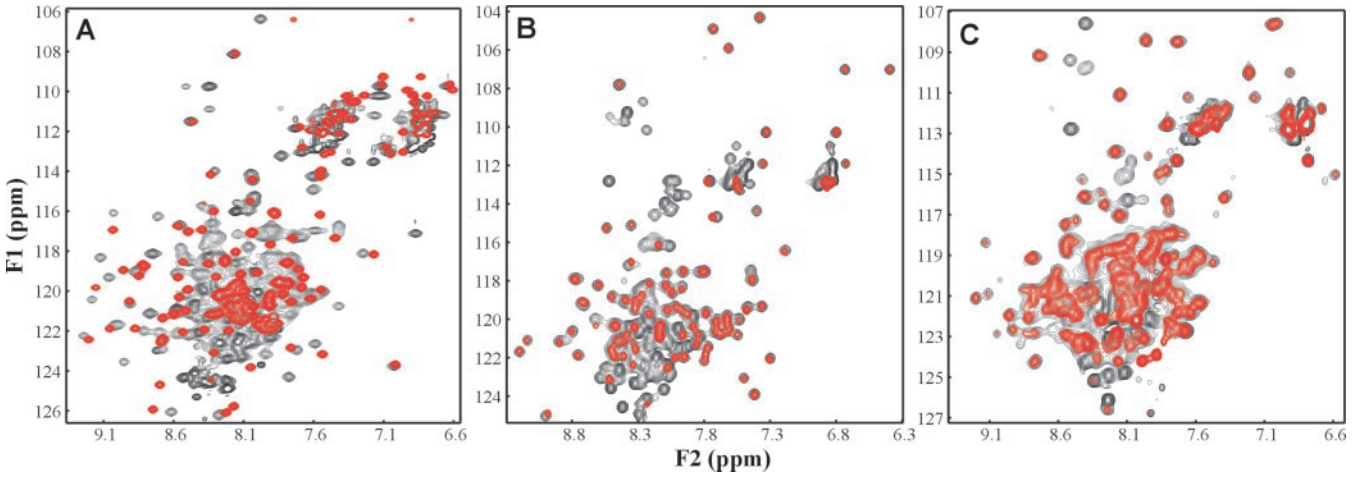

FIG. 3. **Syntaxin 7 forms a closed conformation, but vti1b and syntaxin 8 do not.** *A–C*, superimposed ^{1}H-^{15}N HSQC spectra of the full cytoplasmic region (*black contours*) or the N-terminal domain (*red contours*) of syntaxin 7 (*A*), vti1b (*B*), and syntaxin 8 (*C*).

can be considered as protein fingerprints that contain one cross-peak for each non-proline residue in the sequence. In addition, we assigned the backbone resonances of selected fragments using HNCACB, CBCA(CO)NH, and three-dimensional ^{1}H-^{15}N NOESY-HSQC spectra to determine the secondary structure of the fragments.

The ^{1}H-^{15}N spectrum of the N-terminal fragment of syntaxin 7 (residues 2–131) exhibited a good chemical shift dispersion characteristic of a domain with a well defined tertiary structure (Fig. 3*A*, *red contours*), supporting the notion that this fragment is autonomously folded. Assignment of the backbone resonances of this fragment and comparison of the observed Cα chemical shifts with those expected for a random coil (Fig. 4*A*) showed that the domain contains three α-helices. This conclusion was further confirmed by the observed NOE patterns (data not shown). Analysis of ^{13}C chemical shift indices (38) derived from the data indicate that the helices span approximately residues 11–37, 46–75, and 83–117 of syntaxin 7. The third helix, which appears to be longer, may be extending beyond the limits of the domain because of a helix-nucleating effect toward the C-terminal residues of the fragment. Comparison of the ^{1}H-^{15}N spectrum of the syntaxin 7 N-terminal fragment with that of its full cytoplasmic region (residues 2–235) revealed shifts for many of the cross-peaks from residues 2–131 (Fig. 3*A*, *black contours*), providing clear evidence for an interaction between the N-terminal three-helix bundle and the SNARE motifs. We conclude that the three-helix N-terminal domain of syntaxin 7 folds back onto the SNARE motif to form a closed conformation.

A similar analysis of the N-terminal domain of vti1b (residues 1–124) yielded a well dispersed ^{1}H-^{15}N HSQC spectrum characteristic of a folded domain (Fig. 3*B*, *red contours*). After assigning the backbone resonances of this fragment, the observed downfield shifts of its Cα carbons (Fig. 4*B*) also suggested the presence of three α-helices. The helices span residues 9–33, 38–65, and 72–98 according to the calculated chemical shift indices (38). This result is surprising because proline residues are present at positions 29 and 76. However, the unusually high downfield shifts of the Cα carbons from the residues preceding these two prolines (9.2 ppm for Val-28 and 6.5 ppm for Asn-75), together with the observation of medium range NOEs characteristic of α-helical conformation through the two proline residues, support the conclusion that the first and third helices indeed span residues 9–33 and 72–98, respectively. Hence, our results indicate that vti1b contains a three-helix N-terminal domain that is similar to that of the syntaxins. However, when we compared the ^{1}H-^{15}N HSQC spectrum

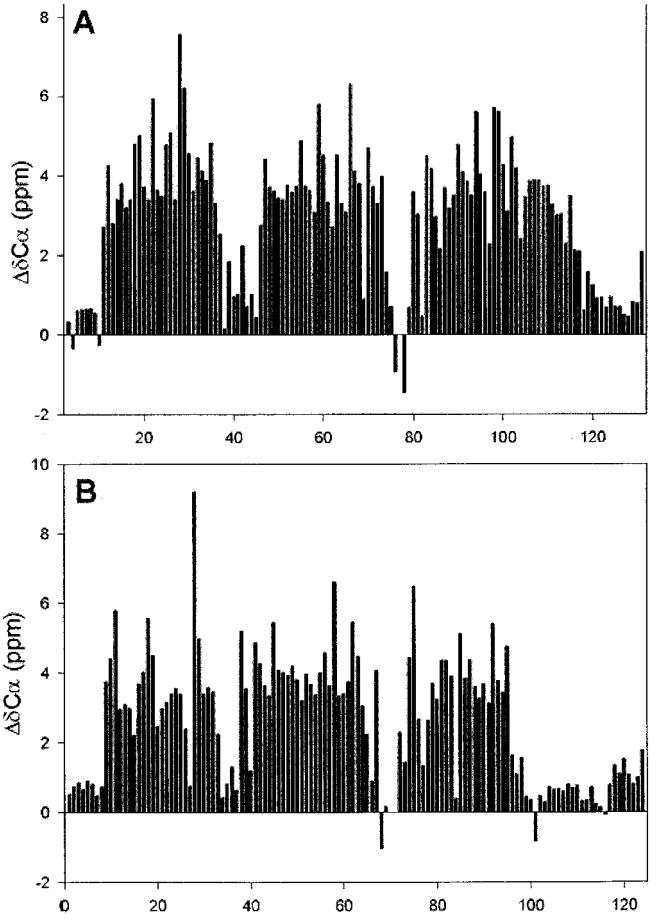

FIG. 4. **Syntaxin 7 and vti1b contain three-helix N-terminal domains.** The differences ($\Delta\delta C\alpha$) between the Cα chemical shifts observed in the N-terminal fragments of syntaxin 7 (*A*) and vti1b (*B*) and those expected for a random coil are plotted as a function of the residue number. Groups of consecutive, large positive values of $\Delta\delta C\alpha$ are characteristic of α-helices. Random coil values were obtained from the BioMagResBank.

of the vti1b N-terminal fragment with that of its full cytoplasmic region (residues 1–206) (Fig. 3*B*, *black contours*), no shifts were observed for the cross-peaks corresponding to residues 1–124. Thus, the N-terminal domain of vti1b does not form a closed conformation. To confirm that this result does not arise from aggregation of the SNARE motif, we also acquired an ^{1}H-^{15}N HSQC spectrum of a fragment corresponding to the

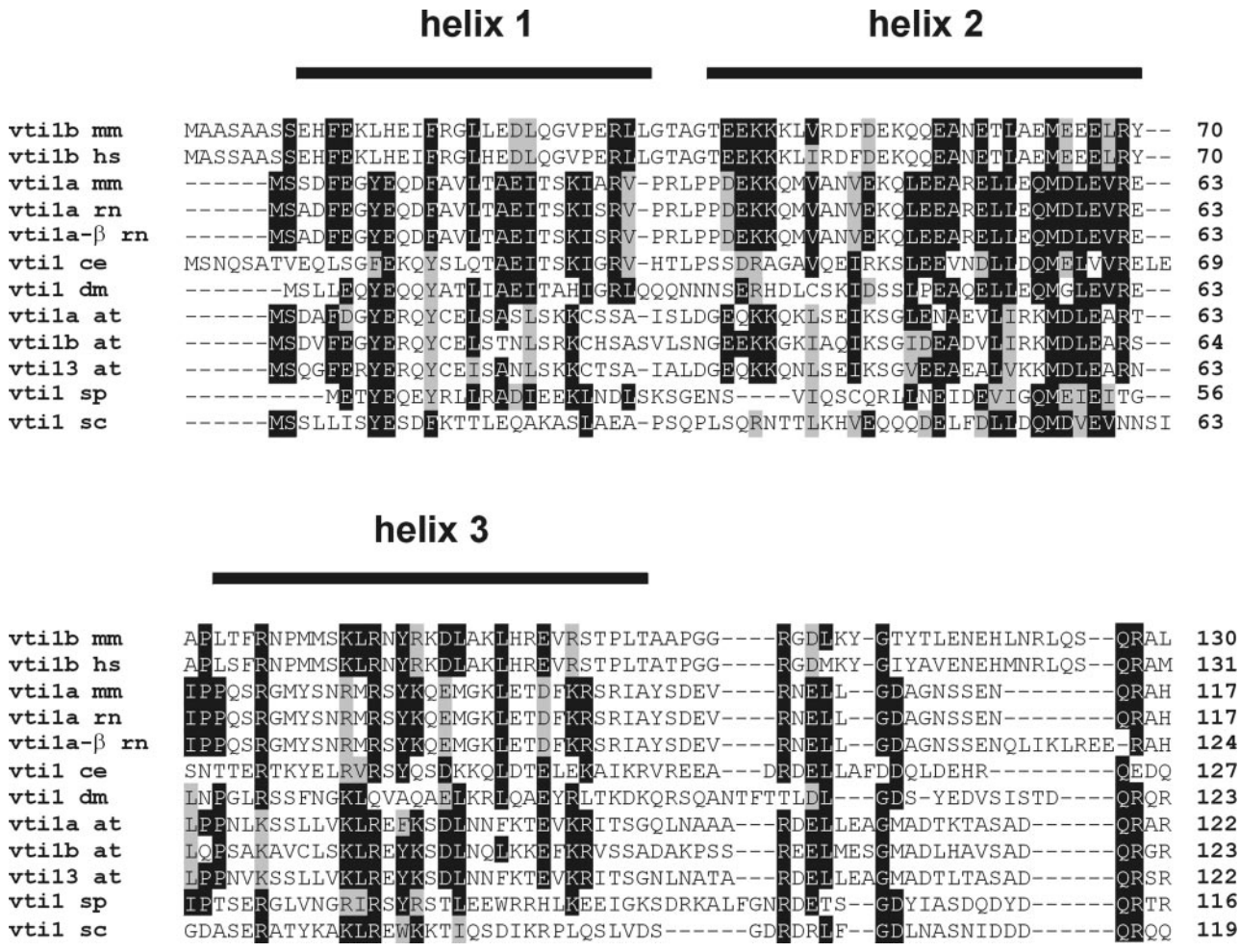

FIG. 5. **Sequence alignment of the N-terminal regions of members of the vti1 family.** Identical (*black boxed*) or highly homologous ((L/I/V), (R/K), (E/D), *gray boxed*) residues that are found in more than 50% (at least 7 out of 12) sequences are *marked*. The regions found to be α-helical in vti1b are marked on *top* of the alignment. GenBank™ accession numbers are AF035209 and AF035208 for mouse (*mm*) vti1a and vti1b, respectively; AF035824 for human vti1b (*hs*); AF262221 and AF262222 for rat (*rn*) vti1a and vti1a-β, respectively; CAB 16506 and AE003469 for vti1 from *C. elegans* (*ce*) and *Drosophila melanogaster* (*dm*), respectively; AF114750, AF114751, and BAB01986 for *Arabidopsis thaliana* (*at*) vti1a, vti1b, and vti13, respectively; AF006074 for vti1 from *Saccharomyces cerevisiae* (*sc*); AL022070 for vti1 from *Schizosaccharomyces pombe* (*sp*).

isolated SNARE motif (residues 130–206). As observed for Vam3p (26), the SNARE motif exhibits sharp cross-peaks with low chemical shift dispersion characteristic of an unfolded polypeptide, and these cross-peaks coincide with sharp cross-peaks from the ^{1}H-^{15}N HSQC spectrum of the full cytoplasmic region (Supplementary material, Fig. 1*A*).

Sequence analysis of the N-terminal domains of members of the vti1 family showed a conservation of residues located within the α-helical regions of vti1b (Fig. 5). This evolutionary conservation of the primary sequence suggests that a three-helix N-terminal domain is a conserved feature of all members of the vti1 family. This suggestion fits well with the finding that yeast vti1 is highly α-helical (37).

The ^{1}H-^{15}N HSQC of the N-terminal domain of syntaxin 8 (residues 1–134) (Fig. 3*C*, *red contours*) was also characteristic of a folded domain. However, the tendency of this domain to aggregate prevented more detailed characterization. Nevertheless, comparison of the ^{1}H-^{15}N HSQC spectrum of this fragment with that of the full cytoplasmic region of syntaxin 8 (residues 1–213) (Fig. 3*C*, *black contours*) revealed no shifts in the cross-peaks from residues 1–134, showing that syntaxin 8 does not adopt a closed conformation. This conclusion was confirmed by comparison of the ^{1}H-^{15}N HSQC spectra of the cytoplasmic region and the isolated SNARE motif of syntaxin 8 (Supplementary material, Fig. 1*B*), which yielded similar results to those obtained for vti1b. Thus, syntaxin 8 appears to have a similar conformational behavior to that of vti1b, but the presence of a three-helix N-terminal domain could not be established from these data. However, the high α-helical content of this domain makes such a conformation very likely. Overall, the NMR data correlate very well with the CD analysis and show that only syntaxin 7 adopts a closed conformation.

The N-terminal Domain of Syntaxin 7 Decreases the Rate of SNARE Complex Assembly—In the final set of experiments, we examined whether the presence of the N-terminal domains influences the assembly kinetics of the endosomal SNARE complex. As outlined in the Introduction, the presence of the N-terminal domain in syntaxin 1 and Sso1p considerably retards SNARE assembly (22, 23). First, we determined the assembly reaction rate of the SNARE motifs, *i.e.* in the absence of the N-terminal domains. To monitor assembly, the four SNARE motifs were mixed. At different time points, aliquots were taken, and the reaction was stopped by adding urea to 4 M, conditions known to freeze the state of assembly (15). For quantification, aliquots were subjected to ion exchange chromatography to separate the monomers from the assembled complex, and the peak integral at 280 nm was determined. As shown in Fig. 6, the core complex forms with a half-time of ~7 h. The slow assembly kinetics is probably due to the fact that nucleation requires the simultaneous contact between four dif-

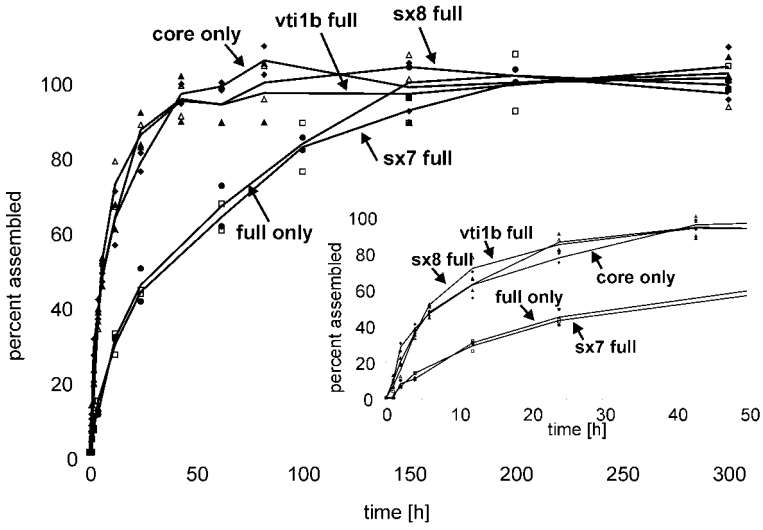

FIG. 6. **Assembly kinetics of different endosomal complexes.** Endosomal complexes containing only the SNARE motifs (*core only*), the N-terminal domain of syntaxin 7 (*sx7 full*), vti1b (*vti1b full*), syntaxin 8 (*sx8 full*), or all three (*full only*) were assembled by mixing the individual components. At indicated time points, aliquots were removed, and the percentage of assembled complex was determined. *Lines* are the average of the two individual points for each complex. *Inset* shows early time points of the kinetics.

ferent proteins in a suitable conformation. When instead of the SNARE motifs of vti1b and syntaxin 8 the full cytoplasmic regions of these SNAREs (vti1bfull and sx8full, respectively) were employed, no change in the assembly kinetics was observed. However, when the SNARE motif of syntaxin 7 was replaced by the full cytoplasmic region, the assembly kinetics was retarded by a factor of 7 (Fig. 6). The same rate was measured when the cytoplasmic domains of all SNAREs were used, supporting the theory that the N-terminal domains of vti1b and syntaxin 8 do not influence assembly. Similar data were obtained when assembly kinetics was measured with different techniques including CD spectroscopy, fluorescence anisotropy, and complex separation by non-denaturing gels (data not shown). We conclude that in the endosomal SNARE complex assembly is only influenced by the N-terminal domain of syntaxin 7, which correlates with its ability to adopt a closed conformation.

DISCUSSION

In the present study, we have analyzed the N-terminal regions of the endosomal SNAREs syntaxin 7, syntaxin 8, and vti1b using biophysical techniques. All three regions contain well folded α-helical domains. In syntaxin 7 and vti1b, they constitute three-helix bundles similar to those determined previously for syntaxin1, Sso1p, and Vam3p. For the N-terminal domain of syntaxin 8, a similar fold is likely, but no certain conclusion can be drawn from our data. Furthermore, we found that among these SNAREs, only syntaxin 7 adopts a closed conformation, which is corroborated by the fact that only the presence of the syntaxin 7 N-terminal domain retards assembly of the endosomal SNARE complex.

A three-helix bundle N-terminal domain has been found in all syntaxins whose domain structures have been analyzed in detail, including the neuronal syntaxin 1 (17) and the yeast Sso1p (21), Vam3p (26), and Sed5p (27). However, the presence of such a domain is generally difficult to establish from sequence analysis alone due to high divergence in this region among syntaxins that function in different cellular compartments. In addition, the length of the helices varies from one syntaxin to another (*e.g.* ~35 residues for syntaxin 1 *versus* ~26 residues for Vam3p), and prolines are sometimes found in the middle of the helices (26), which further hinders the reliable prediction of the location of the helices. Syntaxin 7 is a "true" syntaxin (a Qa-SNARE, (9, 10)) and represents the sixth protein in this SNARE subclass whose N-terminal domain forms a three-helix bundle. Thus, this result further reinforces the notion that all syntaxins contain this domain.

Surprisingly, the N terminus of the SNAP-25 relative vti1b (a Qb-SNARE) is also represented by a three-helical bundle. This is the first SNARE found to contain this type of domain outside the syntaxin family, and sequence alignments suggest that this structure is conserved throughout evolution among the members of the vti1-subfamily. The observation that a non-syntaxin SNARE also contains an evolutionarily conserved N-terminal three-helix bundle suggests that this is a predominant structure in SNARE N-terminal domains not restricted to a particular subfamily.

Although structurally conserved, there is so far no coherent picture concerning the molecular interactions of the N-terminal three-helix bundles. When the free cytoplasmic domains are studied, Sso1p, syntaxin 1, and syntaxin 7 are also closed, whereas Vam3p and vti1b are open. The prevalence of a closed conformation correlates with the retardation of SNARE assembly, both in solution assembly and in liposome fusion assays. Syntaxin 7 is the first syntaxin adopting a closed conformation that does not function at the plasma membrane. Therefore our data show that a closed conformation is not a special feature of exocytotic syntaxins.

It remains unclear to which extent Sec1/Munc-18 proteins regulate the equilibrium between open and closed conformations. Binding of Munc-18 to neuronal syntaxin 1 comprises the best studied example. In this case, binding locks syntaxin in the closed conformation and prevents its interaction with other SNAREs (19, 21, 39). Conversely, Munc-18 does not bind to the assembled synaptic SNARE complex. In contrast, the yeast homologue Sec1p does not bind to isolated Sso1p but rather to the assembled SNARE complex of Sso1/2p, Sec9p, and Snc1/2p (32).

Despite this apparent variability in the interactions involving SNARE N-terminal domains, it is becoming apparent that these domains are crucial for function. For instance, in *Caenorhabditis elegans*, syntaxin mutants that are locked in the open configuration can compensate for a loss of the presynaptic protein Unc13, whereas wild-type syntaxin is inefficient (40). In addition, the N-terminal domain of Sso1p is required for cell viability (21). However, more work is required to determine whether these N-terminal domains perform a common function in most SNAREs or whether they represent functionally heterogeneous adaptive modules that act at different stages of the SNARE conformational and functional cycles. The presence of differently structured N termini in some SNAREs supports the idea that SNAREs are modular proteins, with the SNARE motif being the structurally and functionally common denom-

inator, whereas the N-terminal domains suit specific needs of individual SNAREs. In this context, it should be noted that the yeast SNAP-25 homologue Sec9p possesses a much larger N-terminal domain of unknown structure that, however, appears to be functionally expendable (41). Similarly, the neuron-specific soluble R-SNARE tomosyn possesses an N-terminal domain of unknown function that is 10 times the size of the SNARE motif. Except for Sec1/Munc-18 proteins and the adjacent SNARE motifs, no ligands are known for any of these domains. Undoubtedly, further research will be required to unravel common denominators and specific features of the N-terminal domains of SNARE proteins, and additional twists and turns are likely to appear in this research.

Acknowledgments—We thank Dirk Fasshauer for critical discussion and the hint for adding 4 M urea to freeze the assembly state of a SNARE complex and Tom Südhof for providing the cDNA of human syntaxin 7.

REFERENCES

1. Rothman, J. E. (1994) *Nature* **372,** 55–63
2. Nichols, B. J., and Pelham, H. R. (1998) *Biochim. Biophys. Acta* **1404,** 9–31
3. Jahn, R., and Südhof, T. C. (1999) *Annu. Rev. Biochem.* **68,** 863–911
4. Fasshauer, D., Otto, H., Eliason, W. K., Jahn, R., and Brunger, A. T. (1997) *J. Biol. Chem.* **272,** 28036–28041
5. Fasshauer, D., Eliason, W. K., Brunger, A. T., and Jahn, R. (1998) *Biochemistry* **37,** 10354–10362
6. Hanson, P. I., Heuser, J. E., and Jahn, R. (1997) *Curr. Opin. Neurobiol.* **7,** 310–315
7. Fasshauer, D., Sutton, R. B., Brunger, A. T., and Jahn, R. (1998) *Proc. Natl. Acad. Sci. U. S. A.* **95,** 15781–15786
8. Antonin, W., Fasshauer, D., Becker, S., Jahn, R., and Schneider, T. R. (2002) *Nat. Struct. Biol.* **9,** 107–111
9. Antonin, W., Holroyd, C., Fasshauer, D., Pabst, S., Von Mollard, G. F., and Jahn, R. (2000) *EMBO J.* **19,** 6453–6464
10. Bock, J. B., Matern, H. T., Peden, A. A., and Scheller, R. H. (2001) *Nature* **409,** 839–841
11. Fasshauer, D., Antonin, W., Margittai, M., Pabst, S., and Jahn, R. (1999) *J. Biol. Chem.* **274,** 15440–15446
12. Yang, B., Gonzalez, L., Jr., Prekeris, R., Steegmaier, M., Advani, R. J., and Scheller, R. H. (1999) *J. Biol. Chem.* **274,** 5649–5653
13. McNew, J. A., Parlati, F., Fukuda, R., Johnston, R. J., Paz, K., Paumet, F., Sollner, T. H., and Rothman, J. E. (2000) *Nature* **407,** 153–159
14. Poirier, M. A., Hao, J. C., Malkus, P. N., Chan, C., Moore, M. F., King, D. S., and Bennett, M. K. (1998) *J. Biol. Chem.* **273,** 11370–11377
15. Fasshauer, D., Antonin, W., Subramaniam, V., and Jahn, R. (2002) *Nat. Struct. Biol.* **9,** 144–151
16. Weber, T., Zemelman, B. V., McNew, J. A., Westermann, B., Gmachl, M., Parlati, F., Sollner, T. H., and Rothman, J. E. (1998) *Cell* **92,** 759–772
17. Fernandez, I., Ubach, J., Dulubova, I., Zhang, X., Südhof, T. C., and Rizo, J. (1998) *Cell* **94,** 841–849
18. Lerman, J. C., Robblee, J., Fairman, R., and Hughson, F. M. (2000) *Biochemistry* **39,** 8470–8479
19. Dulubova, I., Sugita, S., Hill, S., Hosaka, M., Fernandez, I., Südhof, T. C., and Rizo, J. (1999) *EMBO J.* **18,** 4372–4382
20. Fiebig, K. M., Rice, L. M., Pollock, E., and Brunger, A. T. (1999) *Nat. Struct. Biol.* **6,** 117–123
21. Munson, M., Chen, X., Cocina, A. E., Schultz, S. M., and Hughson, F. M. (2000) *Nat. Struct. Biol.* **7,** 894–902
22. Nicholson, K. L., Munson, M., Miller, R. B., Filip, T. J., Fairman, R., and Hughson, F. M. (1998) *Nat. Struct. Biol.* **5,** 793–802
23. Parlati, F., Weber, T., McNew, J. A., Westermann, B., Sollner, T. H., and Rothman, J. E. (1999) *Proc. Natl. Acad. Sci. U. S. A.* **96,** 12565–12570
24. Misura, K. M., Scheller, R. H., and Weis, W. I. (2000) *Nature* **404,** 355–362
25. Verhage, M., Maia, A. S., Plomp, J. J., Brussaard, A. B., Heeroma, J. H., Vermeer, H., Toonen, R. F., Hammer, R. E., van den Berg, T. K., Missler, M., Geuze, H. J., and Südhof, T. C. (2000) *Science* **287,** 864–869
26. Dulubova, I., Yamaguchi, T., Wang, Y., Südhof, T. C., and Rizo, J. (2001) *Nat. Struct. Biol.* **8,** 258–264
27. Yamaguchi, T., Dulubova, I., Min, S. W., Chen, X., Rizo, J., and Südhof, T. C. (2002) *Dev. Cell* **2,** 295–305
28. Cheever, M. L., Sato, T. K., de Beer, T., Kutateladze, T. G., Emr, S. D., and Overduin, M. (2001) *Nat. Cell. Bio.* **3,** 613–618
29. Lu, J., Garcia, J., Dulubova, I., Südhof, T. C., and Rizo, J. (2002) *Biochemistry* **41,** 5956–5962
30. Gonzalez, L. C., Jr., Weis, W. I., and Scheller, R. H. (2001) *J. Biol. Chem.* **276,** 24203–24211
31. Tochio, H., Tsui, M. M., Banfield, D. K., and Zhang, M. (2001) *Science* **293,** 698–702
32. Carr, C. M., Grote, E., Munson, M., Hughson, F. M., and Novick, P. J. (1999) *J. Cell Biol.* **146,** 333–344
33. Antonin, W., Riedel, D., and von Mollard, G. F. (2000) *J. Neurosci.* **20,** 5724–5732
34. Wessel, D., and Flügge, U. I. (1984) *Anal. Biochem.* **138,** 141–143
35. Laemmli, U. K. (1970) *Nature* **227,** 680–685
36. Chen, Y. H., Yang, J. T., and Chau, K. H. (1974) *Biochemistry* **13,** 3350–3359
37. Tishgarten, T., Yin, F. F., Faucher, K. M., Dluhy, R. A., Grant, T. R., Fischer von Mollard, G., Stevens, T. H., and Lipscomb, L. A. (1999) *Protein Sci.* **8,** 2465–2473
38. Wishart, D. S., and Sykes, B. D. (1994) *J. Biomol. NMR* **4,** 171–180
39. Yang, B., Steegmaier, M., Gonzalez, L. C., Jr., and Scheller, R. H. (2000) *J. Cell Biol.* **148,** 247–252
40. Richmond, J. E., Weimer, R. M., and Jorgensen, E. M. (2001) *Nature* **412,** 338–341
41. Brennwald, P., Kearns, B., Champion, K., Keranen, S., Bankaitis, V., and Novick, P. (1994) *Cell* **79,** 245–258

PROTEIN STRUCTURE AND FOLDING:

The N-terminal Domains of Syntaxin 7 and vti1b Form Three-helix Bundles That Differ in Their Ability to Regulate SNARE Complex Assembly

Wolfram Antonin, Irina Dulubova, Demet Araç, Stefan Pabst, Juliane Plitzner, Josep Rizo and Reinhard Jahn

J. Biol. Chem. 2002, 277:36449-36456.
doi: 10.1074/jbc.M204369200 originally published online July 11, 2002